A Mixed-Potential Model for the Prediction of the Effects of Alpha-Radiolysis, Precipitation and Redox Processes on the Dissolution of Used Nuclear Fuel

by

Fraser King, David W. Shoesmith and Miroslav Kolar

AECL, Whiteshell Laboratories
Pinawa, Manitoba Canada R0E 1L0

This work is funded by Ontario Hydro, Nuclear Waste Management Division
(J.E. Villagran, Project Engineer).

1998 Spent Fuel Workshop, Las Vegas, 18-20 May 1998.

What are we trying to model?

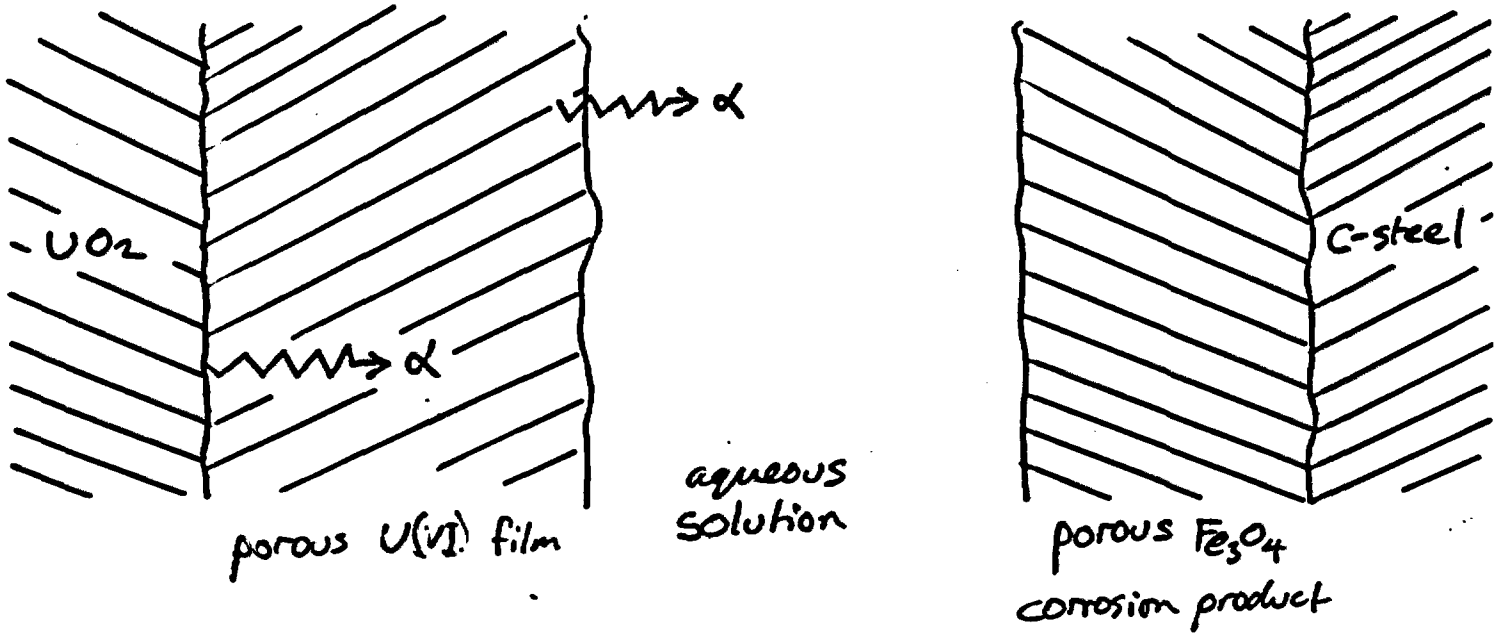

- Summary of existing data on UO_2 electrochemistry

- Outline of mixed-potential model (MPM)
  - reaction scheme
  - reaction-diffusion equations
  - model geometry
  - boundary conditions
  - assumptions

- "Model predictions"
  - validation/verification of MPM
  - effects of α-radiolysis, precipitation and redox processes

Summary of UO_{2+x} Electrochemistry (1)

- Behaves like a p-type semiconductor
- Rates of reaction dependent on potential (E)

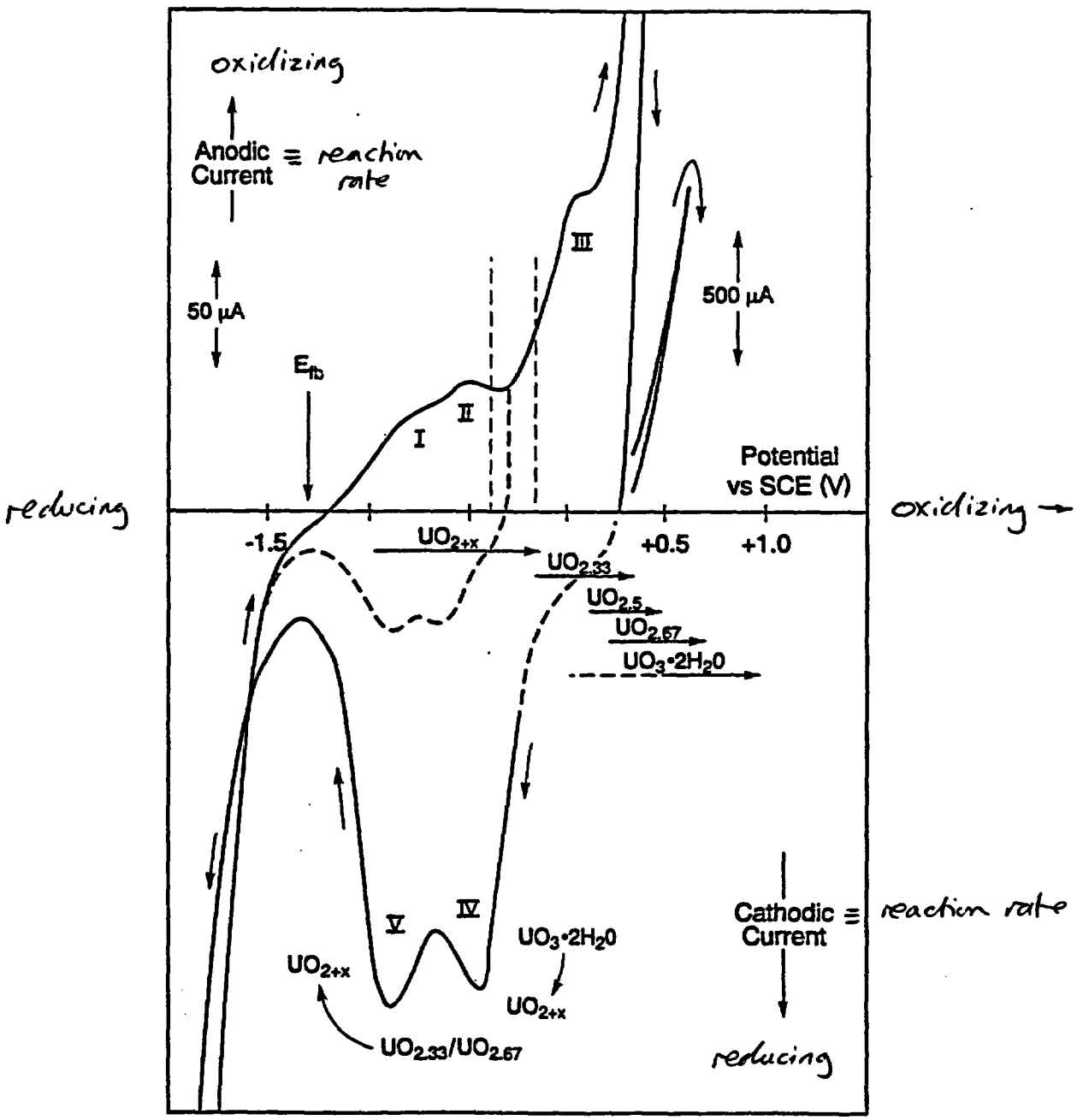

Summary of UO_{2+x} Electrochemistry (2)

- The degree of oxidation of the surface is E dependent
- Above a certain E, dissolution becomes oxidative in nature (i.e., the anodic dissolution to U(VI) is electrochemically coupled to the cathodic reduction of a suitable oxidant).

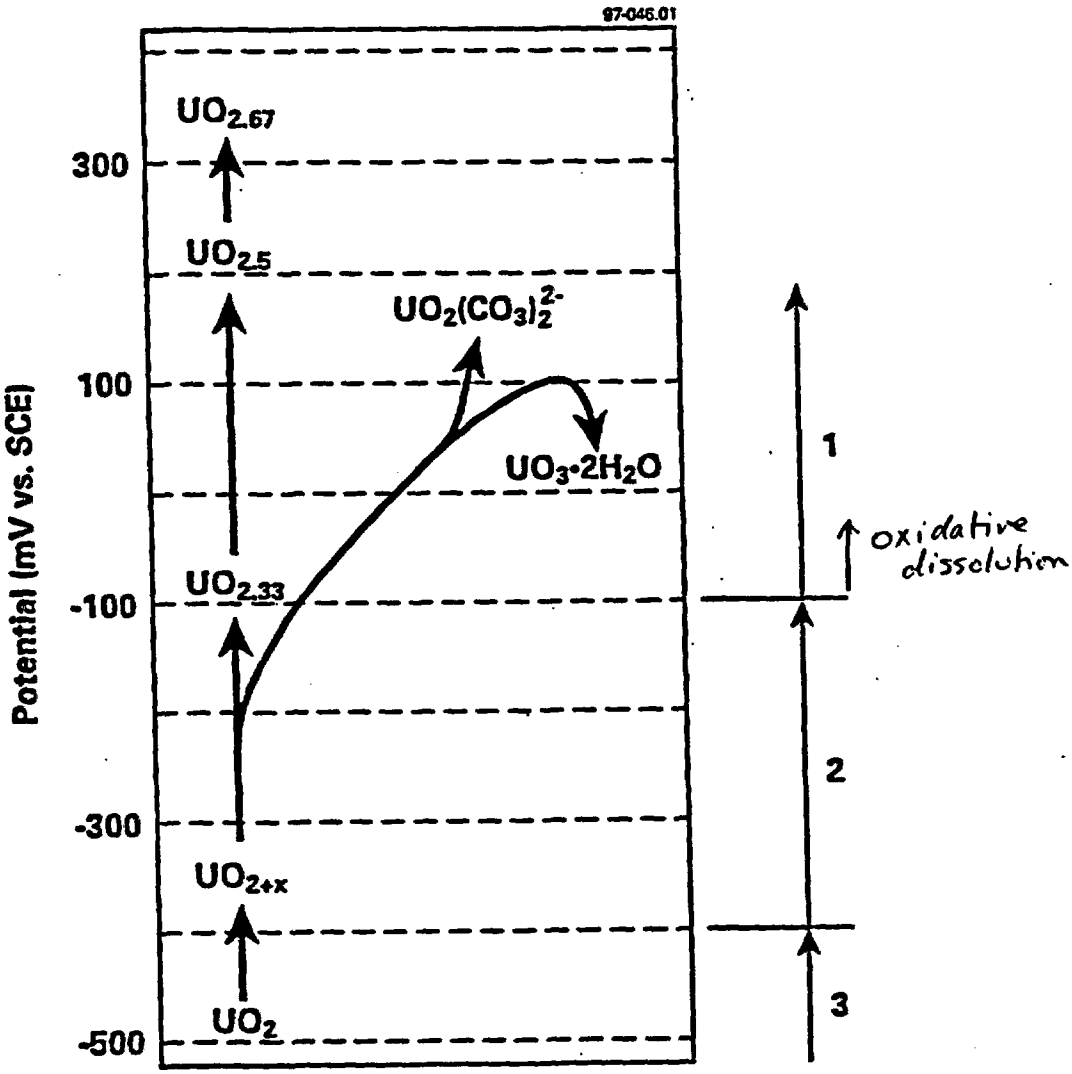

Summary of UO_{2+x} Electrochemistry (3)

- In non-complexing environments, corrosion product films build up on the UO_2 surface, leading to a decrease in the dissolution rate.

pH 9.5, 0.1M $NaClO_4$

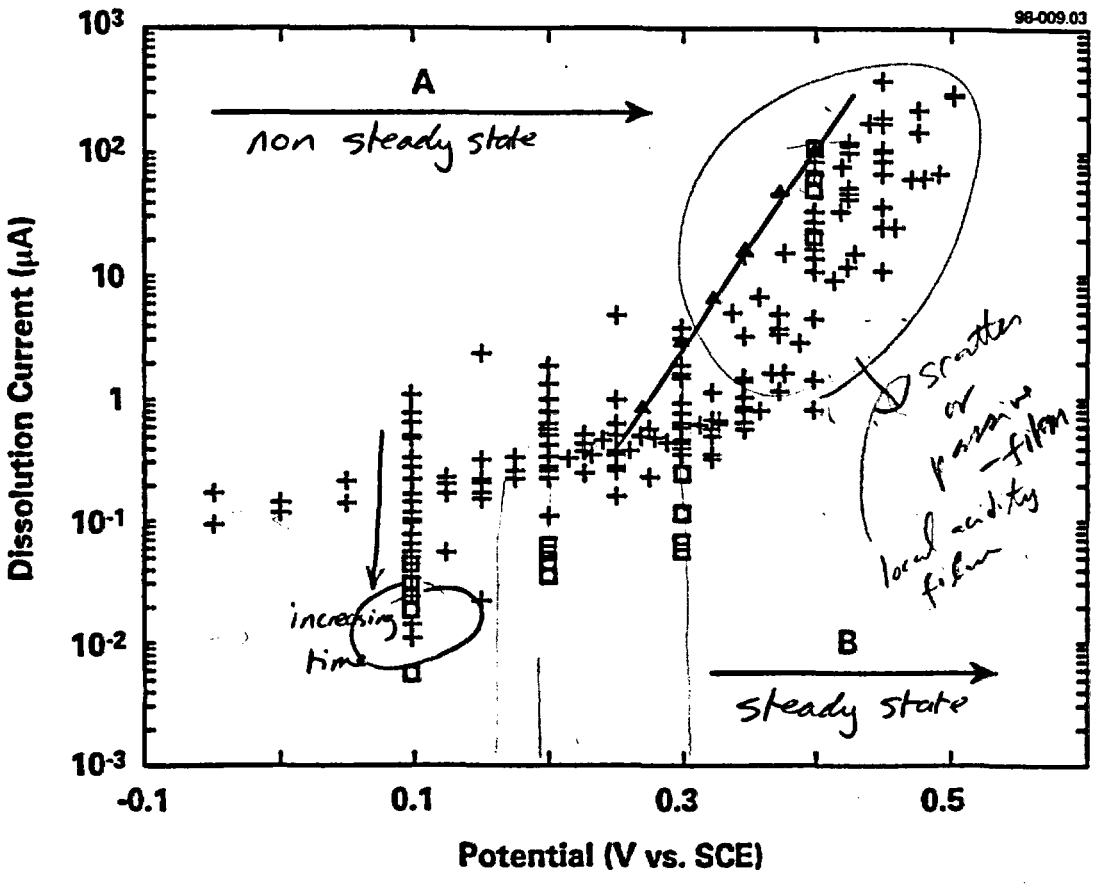

-300 reducing

Summary of UO_{2+x} Electrochemistry (4)

- The addition of complexants for U(VI) increases the rate of dissolution.

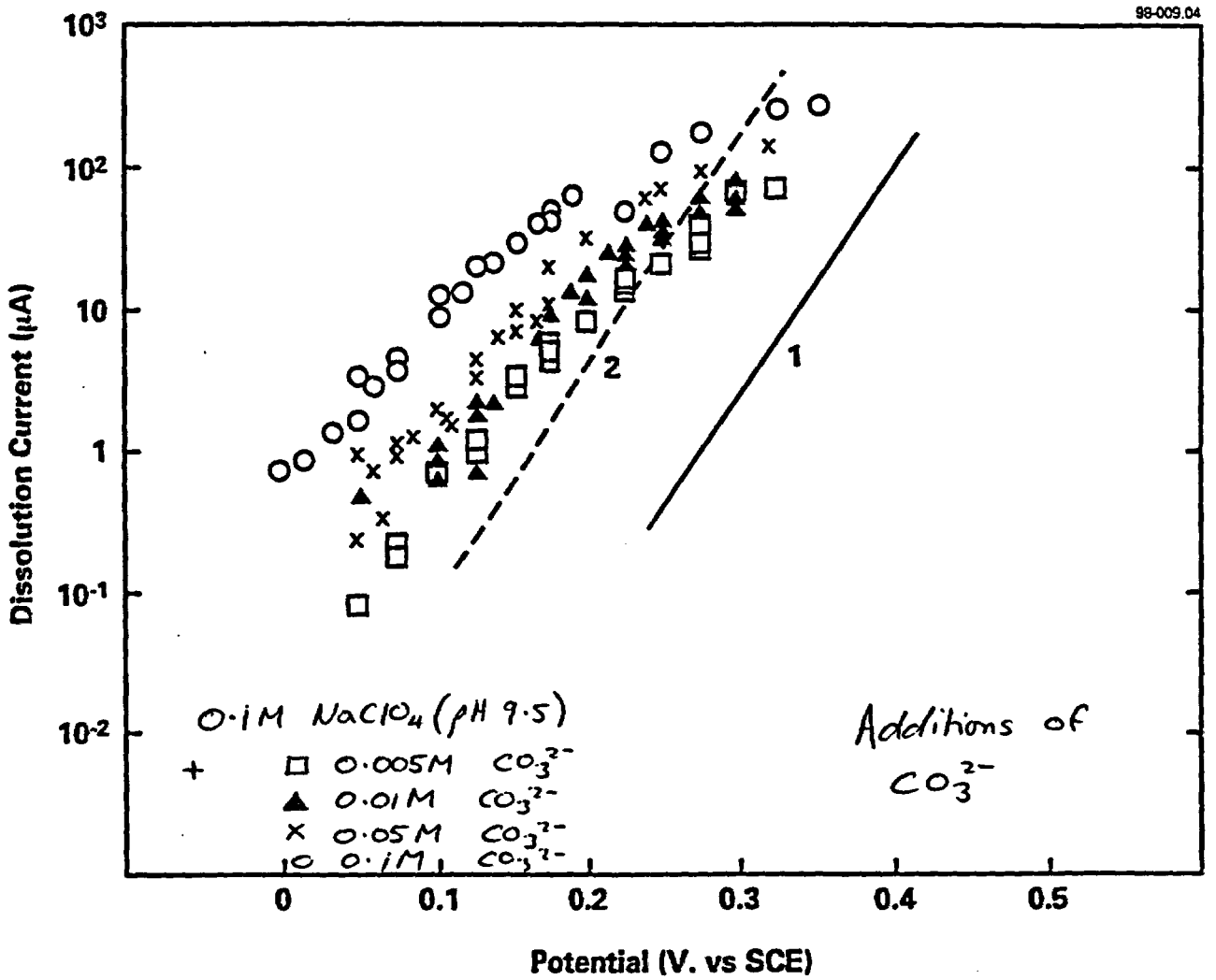

Summary of UO_{2+x} Electrochemistry (5)

- The cathodic reduction of O_2 on UO_2 has been extensively studied.
- Less is known about the cathodic reduction of H_2O_2, or the surface-mediated decomposition of H_2O_2.

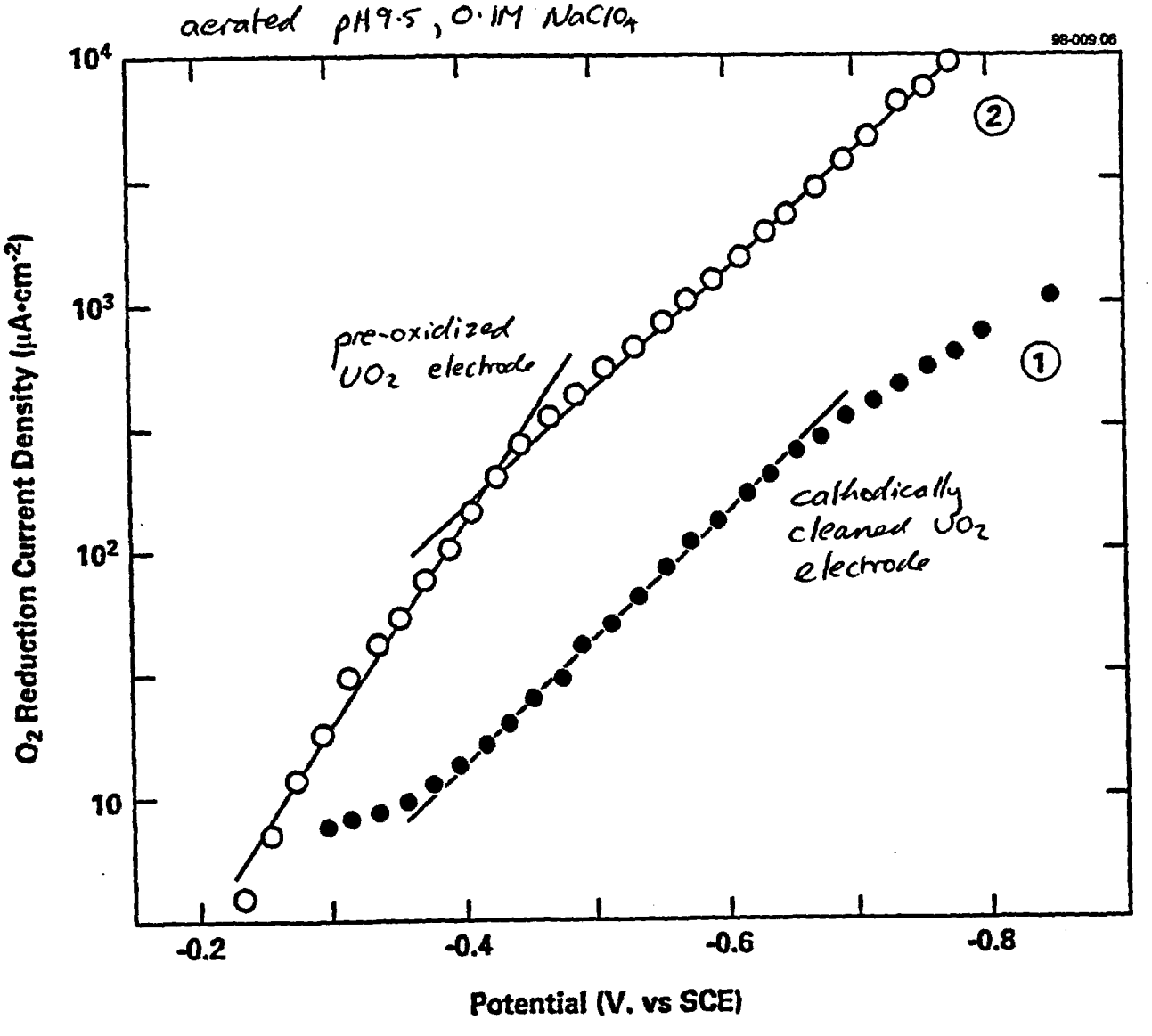

Summary of Electrochemical Data (6)

Potential-Dependent Dissolution Rate of Fe_3O_4

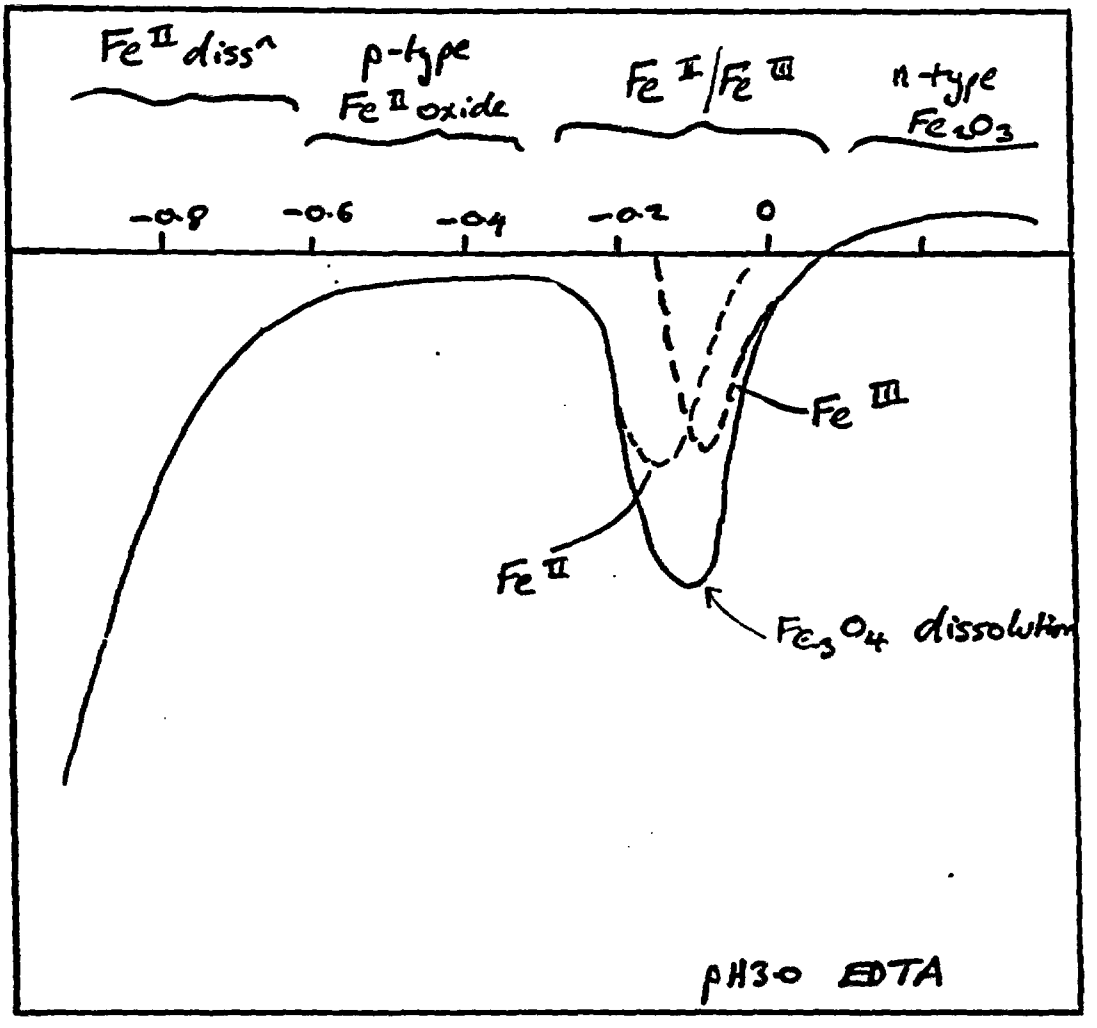

Outline of UO_2 Mixed-Potential Model (1)

The Reaction Scheme

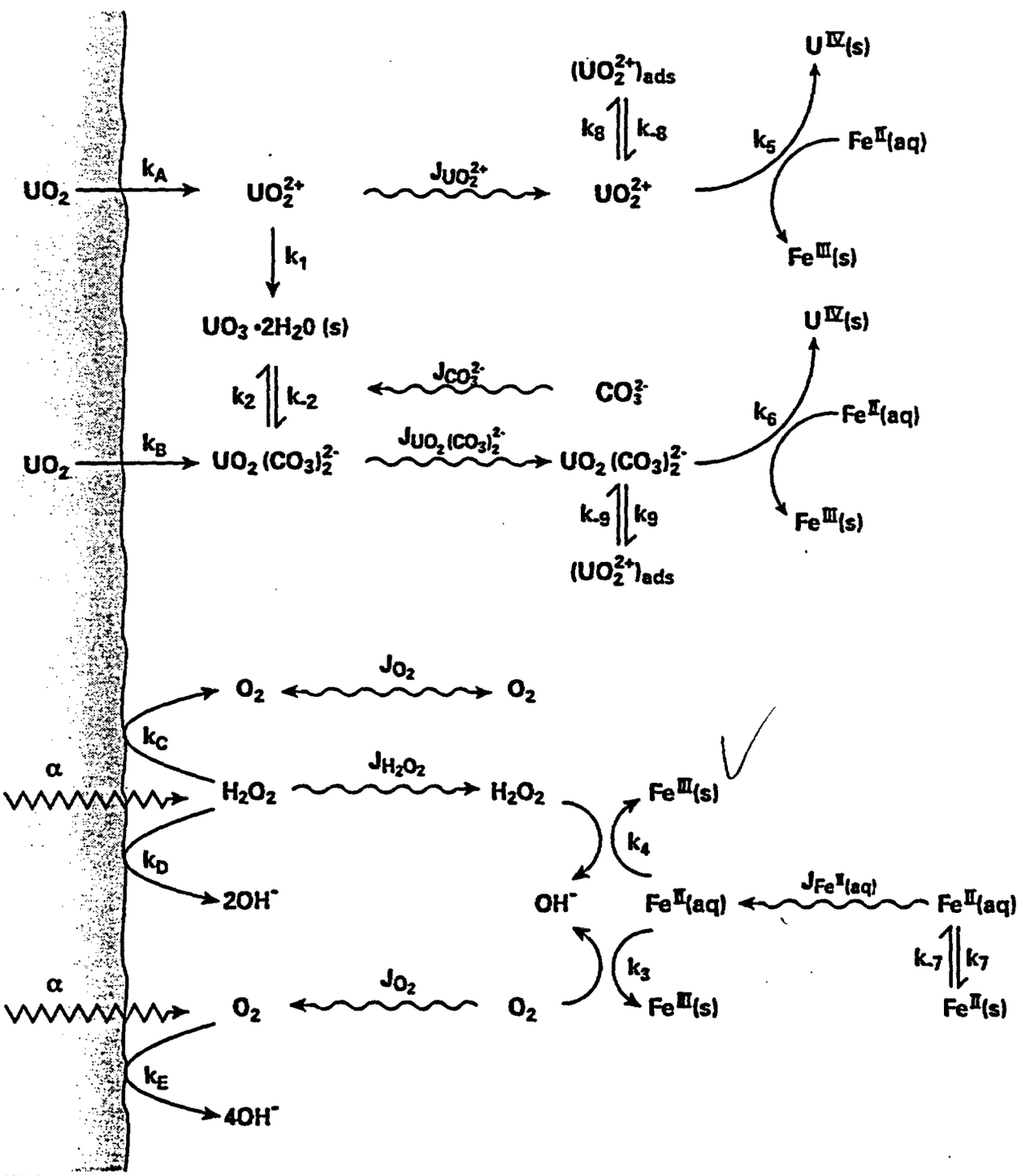

Outline of UO_2 Mixed-Potential Model (2)

The Reaction-Diffusion Equations

The various mass-transport and chemical processes involving the ten species (UO_2^{2+}, $UO_2(CO_3)_2^{2-}$, $UO_3 \cdot 2H_2O(s)$, CO_3^{2-}, O_2, H_2O_2, $Fe(II)_{AQ}$, $Fe(II)_{PPT}$, $U(IV)_{PPT}$ and $UO_2^{2+}(ads)$) are described by reaction-diffusion equations of the general form

$$\varepsilon \frac{\partial c_i}{\partial t} = \frac{\partial}{\partial x}\left(\tau \varepsilon D_i \frac{\partial c_i}{\partial x} \right) + \varepsilon \sum_{j=1}^{9} R_j \qquad \text{for } c = 1,\ldots,10$$

e.g., for O_2 (species #7)

$$\varepsilon \frac{\partial c_7}{\partial t} = \frac{\partial}{\partial x}\left(\tau \varepsilon D_7 \frac{\partial c_7}{\partial x} \right) + G_7 R(x,t) - \varepsilon k_3 c_7 c_9$$

and for $UO_3 \cdot 2H_2O(s)$ (species #3)

$$\varepsilon \frac{\partial c_3}{\partial t} = \varepsilon k_1 \max(0,(c_1 - c_1^{sat}) + \varepsilon k_2 \max(0,(c_2 - c_2^{sat}) - \varepsilon k_{-2} c_3 c_6^p$$

Since D_i and k_j are temperature dependent, we also solve a heat-conduction equation

$$\rho C \frac{\partial T}{\partial t} = \frac{\partial}{\partial x}\left(K \frac{\partial T}{\partial x} \right)$$

to predict T(x,t) and, hence, $D_i(x,t)$ and $k_j(x,t)$ (depending upon model geometry, may assume T(t) only).

Outline of UO_2 MPM (3)

The Spatial Grid

- one-dimensional representation of the container and vault geometries
- two possible model geometries are:

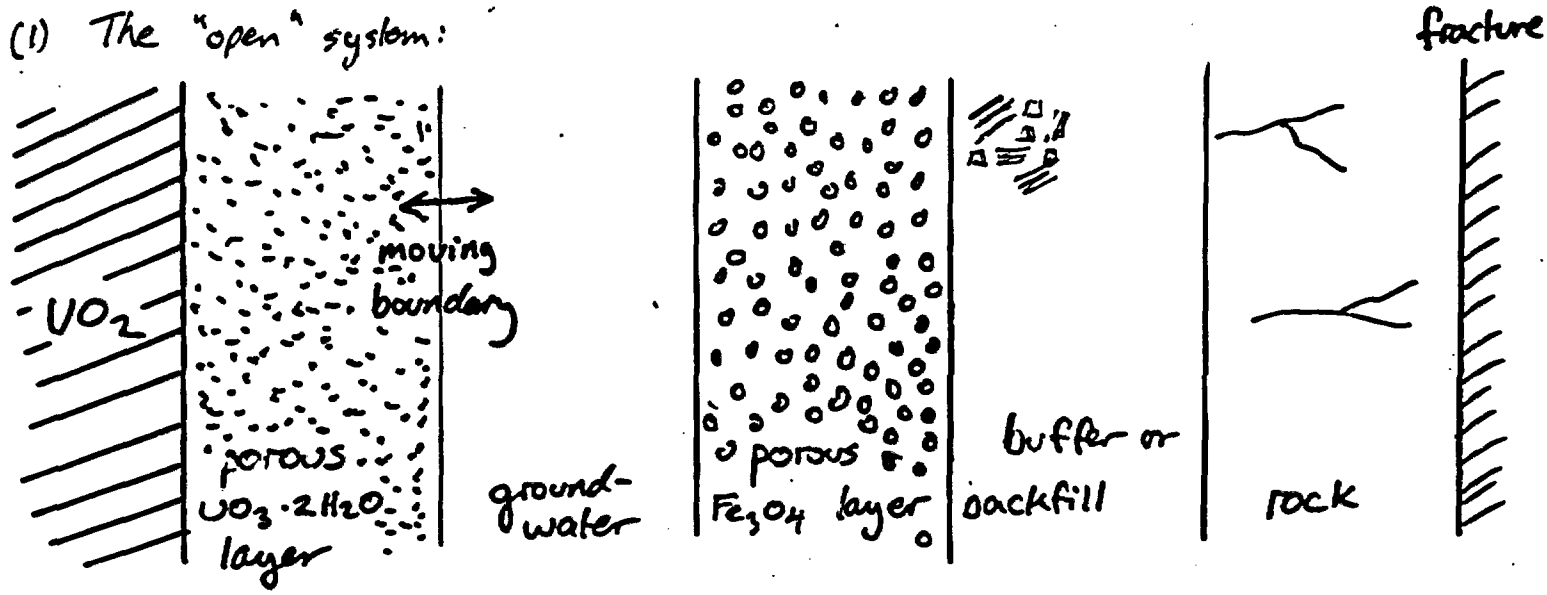

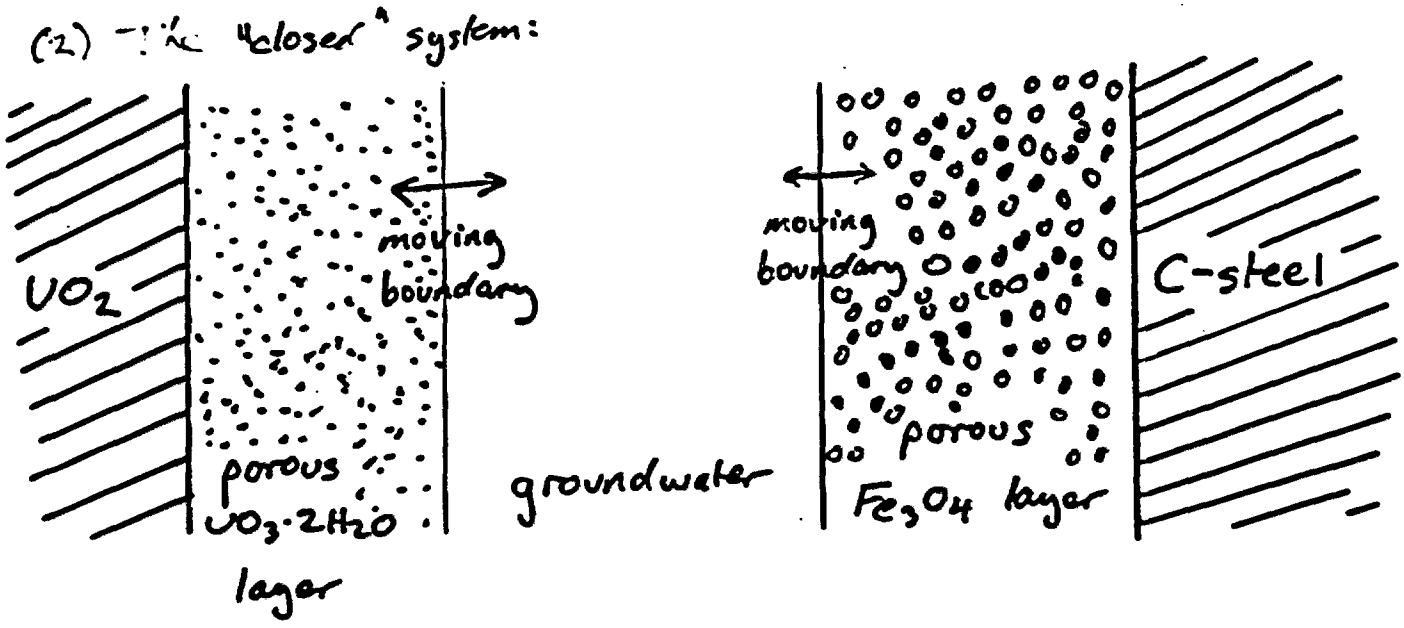

Outline of UO_2 MPM (4)

A Closer Look at the Porous U(VI) Layer

The U(VI) precipitate layer has several effects:

- blocks the surface electrochemical reactions
- inhibits mass transport to and from the UO_2 surface
- affects the yield and location of radiolysis products

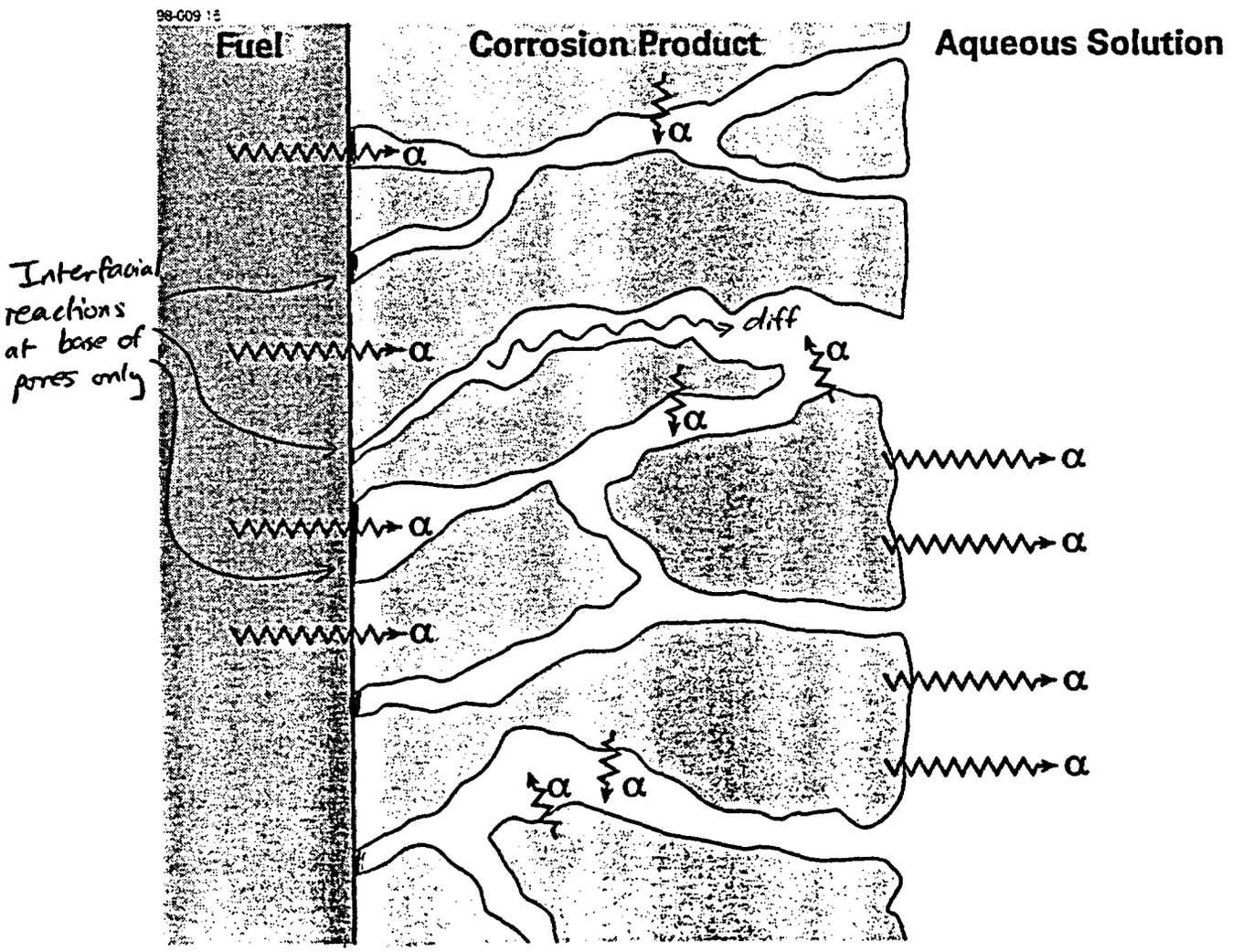

Outline of UO_2 MPM (5)

Boundary Conditions

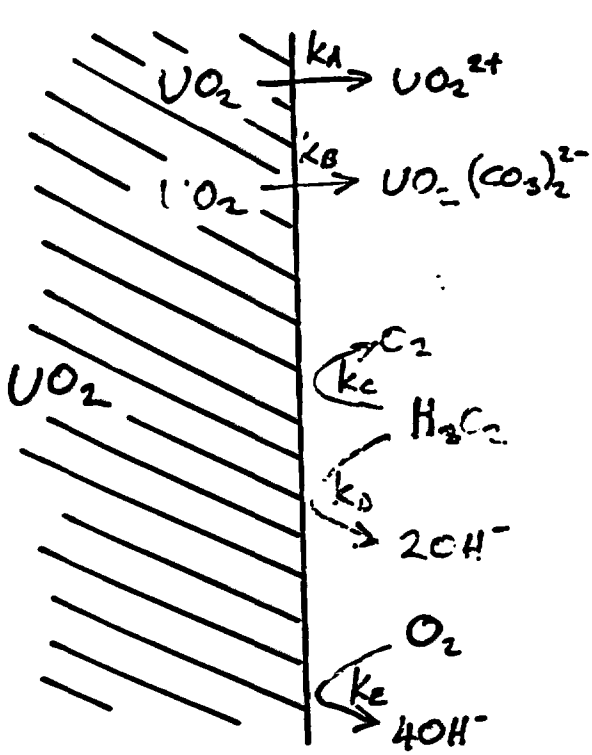

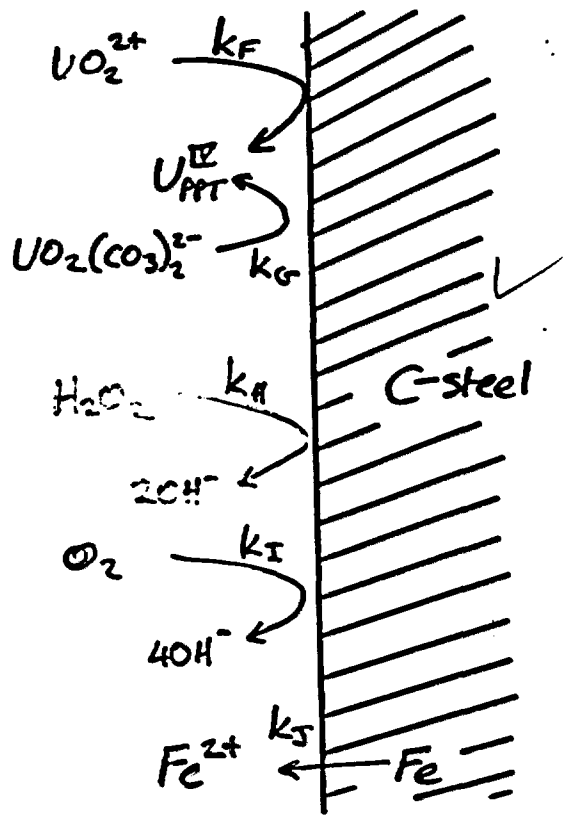

$$I_A + I_B + I_C = -(I_D + I_E)$$

$$I = \pm nF\tau\varepsilon D\frac{\partial c(0,t)}{\partial x}$$

$$I = \pm nF\varepsilon Akc(0,t)\exp\left(\pm\frac{\alpha F}{RT}(E-E^0)\right)$$

Derived parameters:

$$I_{CORR} = I_A + I_B$$

$$E_{CORR} = E_A^0 + \frac{RT}{\alpha_A F}\ln\left\{\frac{I_{CORR}}{2F\varepsilon Ak_A}\right\}$$

$$I_J = -(I_F + I_G + I_H + I_J)$$

$$I = \pm nF\tau\varepsilon' D\frac{\partial c(x_{right},t)}{\partial x}$$

$$I = \pm nF\varepsilon' Akc(x_{right},t)\exp\left(\pm\frac{\alpha F}{RT}(E-E^0)\right)$$

Derived parameters:

$$I_{CORR} = I_J$$

$$E_{CORR} = E_J^0 + \frac{RT}{\alpha_J F}\ln\left\{\frac{I_{CORR}}{2F\varepsilon' Ak_J}\right\}$$

Outline of UO_2 MPM (6)

Assumptions

- the reaction scheme and 1-D model geometry adequately describe the oxidative dissolution of UO_2
- uniform dissolution of the fuel surface (no localized effects, such as gb etching)
- mass transport by diffusion only
- system is completely saturated and the supply of H_2O is not limiting
- no effect of Zircaloy fuel cladding
- effects of α-radiolysis can be simulated by O_2 and H_2O_2 only
- U(VI) and Fe_3O_4 films can be treated as equivalent porous media with spatially and temporally constant porosity and tortuosity
- U(VI) film is assumed to be electrically insulating with electrochemical reactions restricted to base of pores
- U(VI) film attenuates α-dose rate at the fuel surface and contains co-precipitated α-emitters
- film growth occurs at the film/solution interface with no precipitation within the pores
- Fe_3O_4 is the stable C-steel corrosion product
- constant pH throughout the system (pH 7)
- various assumptions involved in derivation of input data

"Model Predictions" (1)

Validation/Verification of the Model

(a)

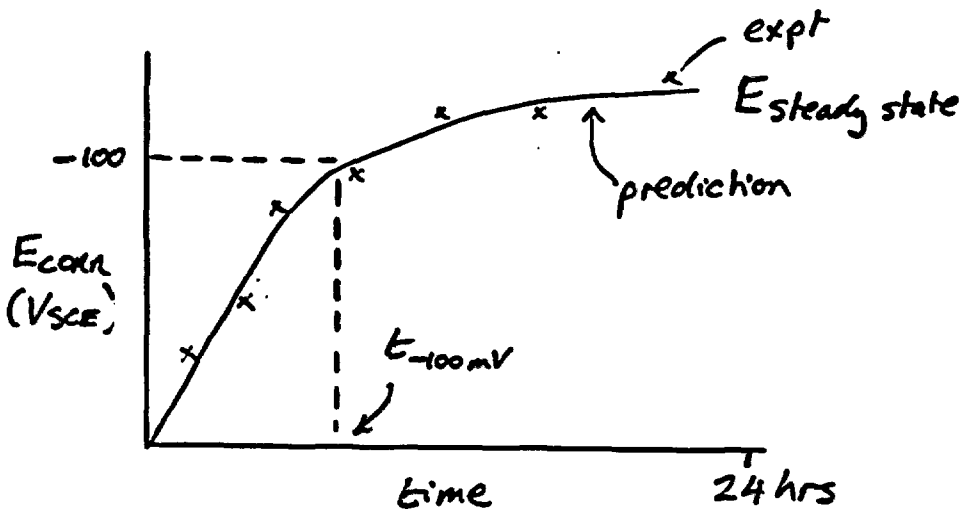

(b)

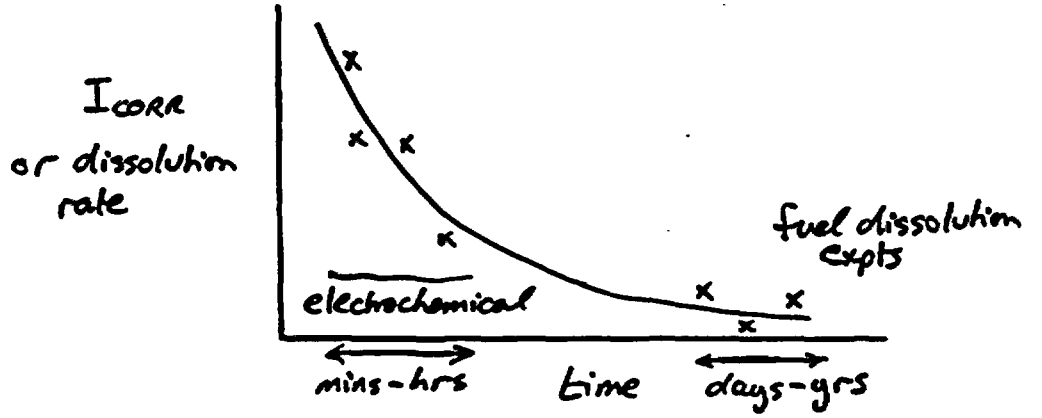

(c)

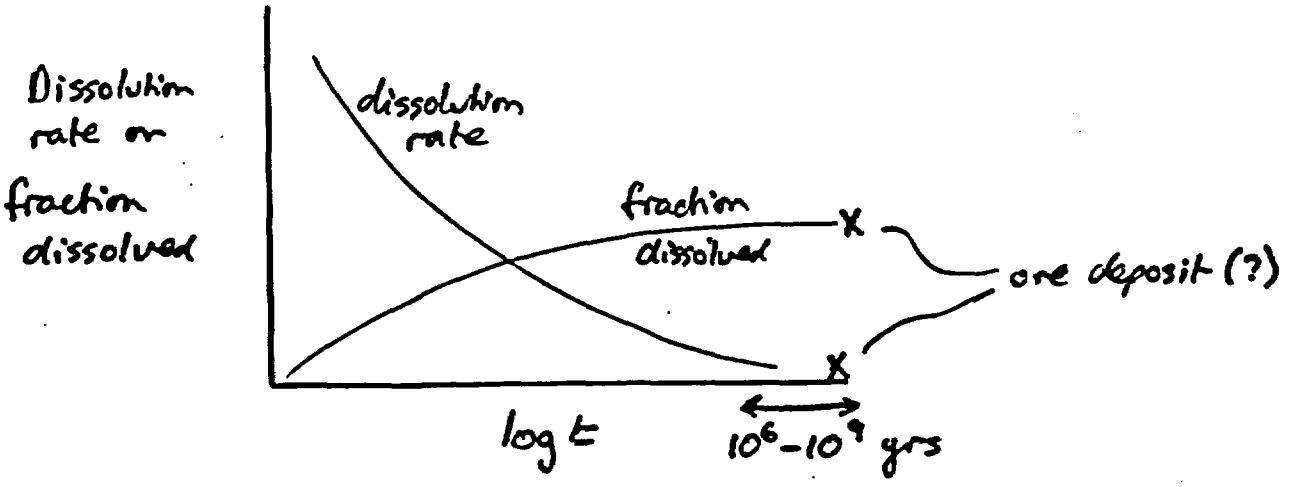

"Model Predictions" (2)

The most basic prediction is of I_{CORR} and E_{CORR} of the UO_2 surface

- I_{CORR} is equivalent to the dissolution rate
- E_{CORR} indicates the period of oxidative dissolution

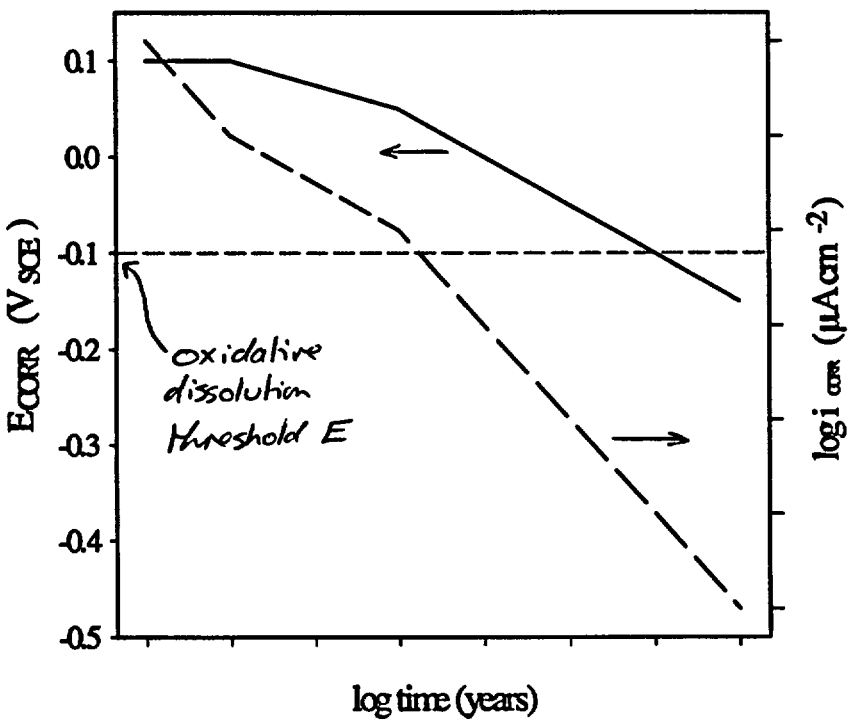

"Model Predictions" (3)

- To what extent does film growth inhibit UO_2 dissolution?

(a)

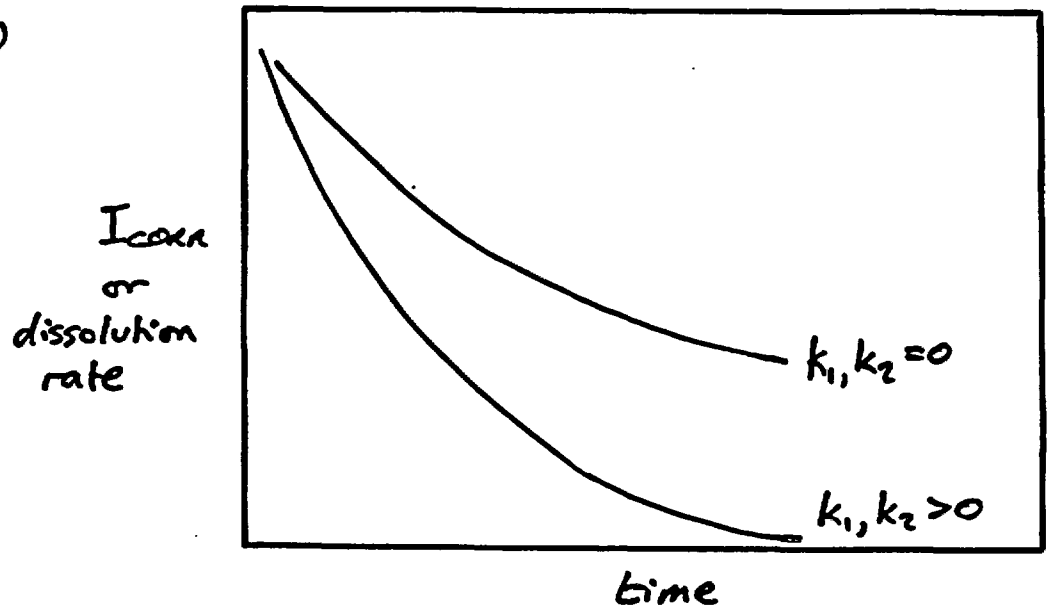

(b)

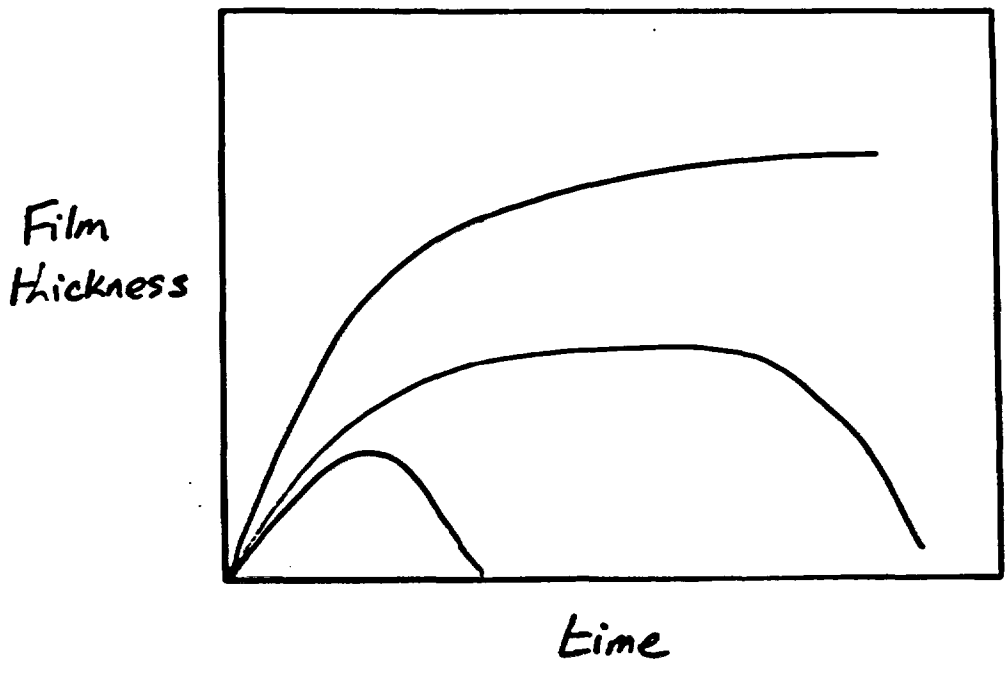

"Model Predictions" (4)

- The ability of the C-steel to act as a redox barrier

(a)

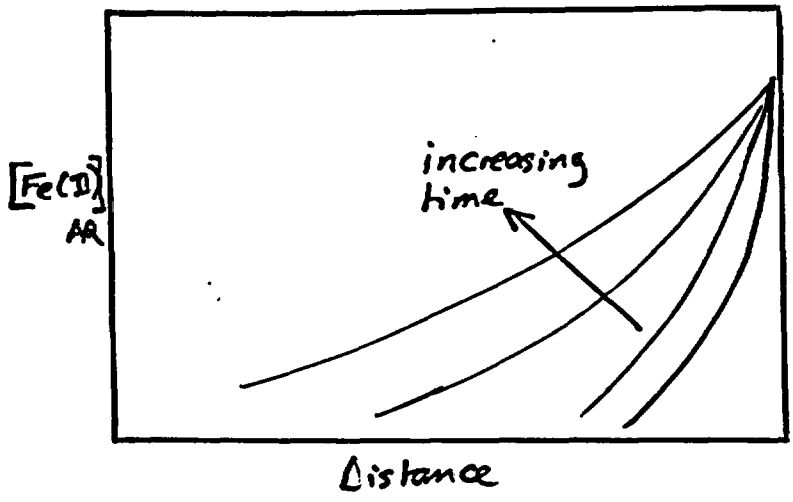

(b)

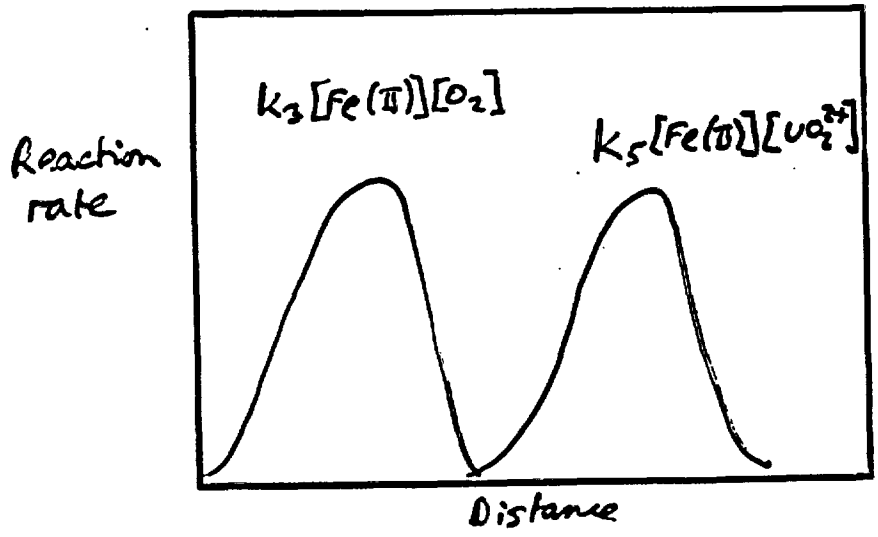

(c)

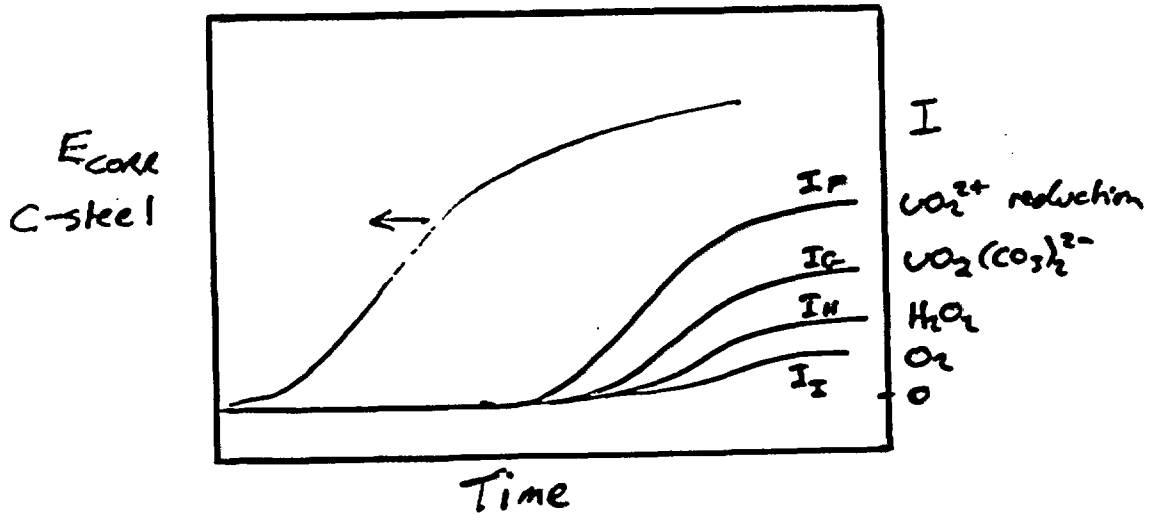

Future Developments (1)

(1) Inclusion of multiple growing layers

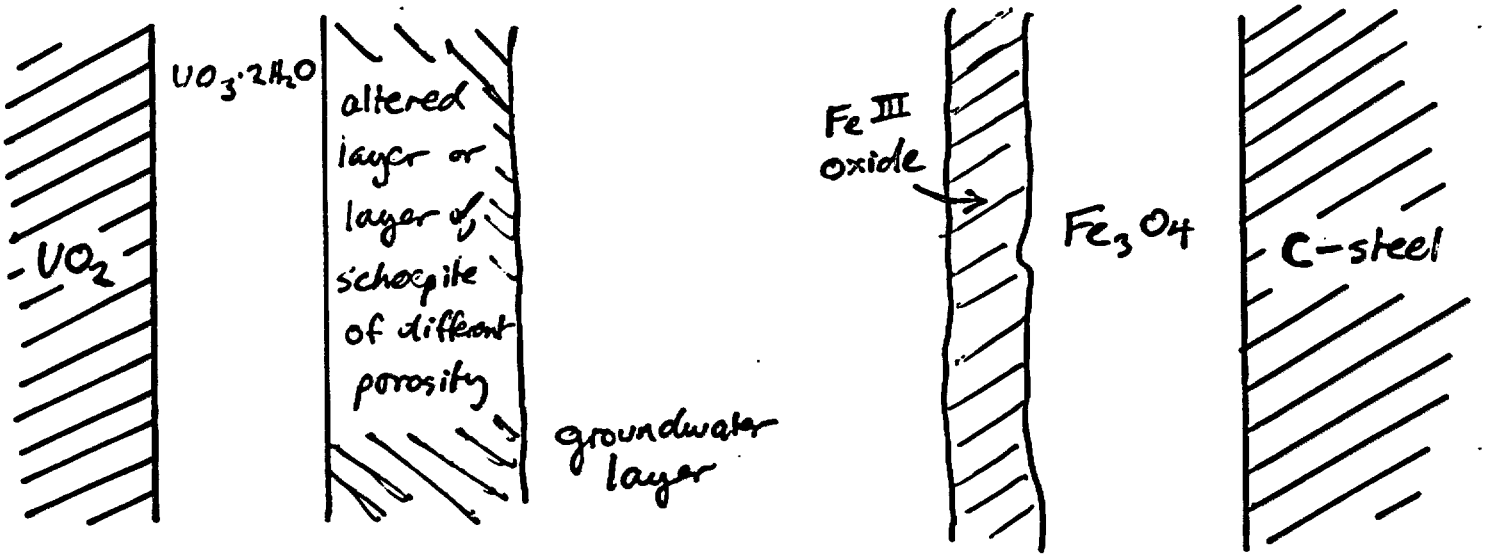

(2) More detailed radiolysis modelling

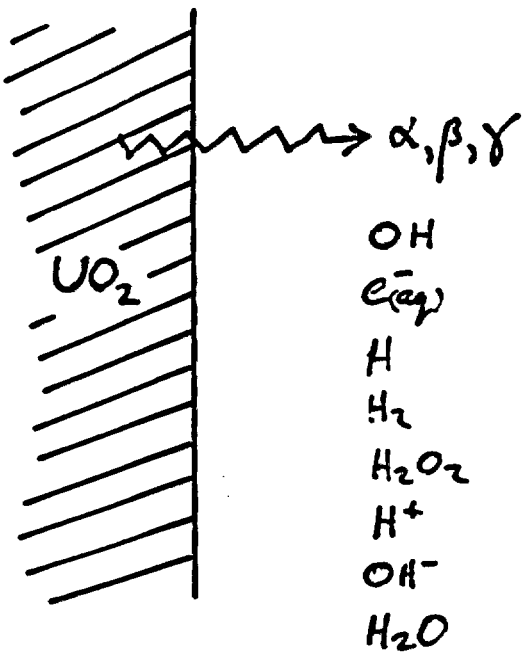

Future Developments (2)

(3) Inclusion of H_2 produced by radiolysis and corrosion

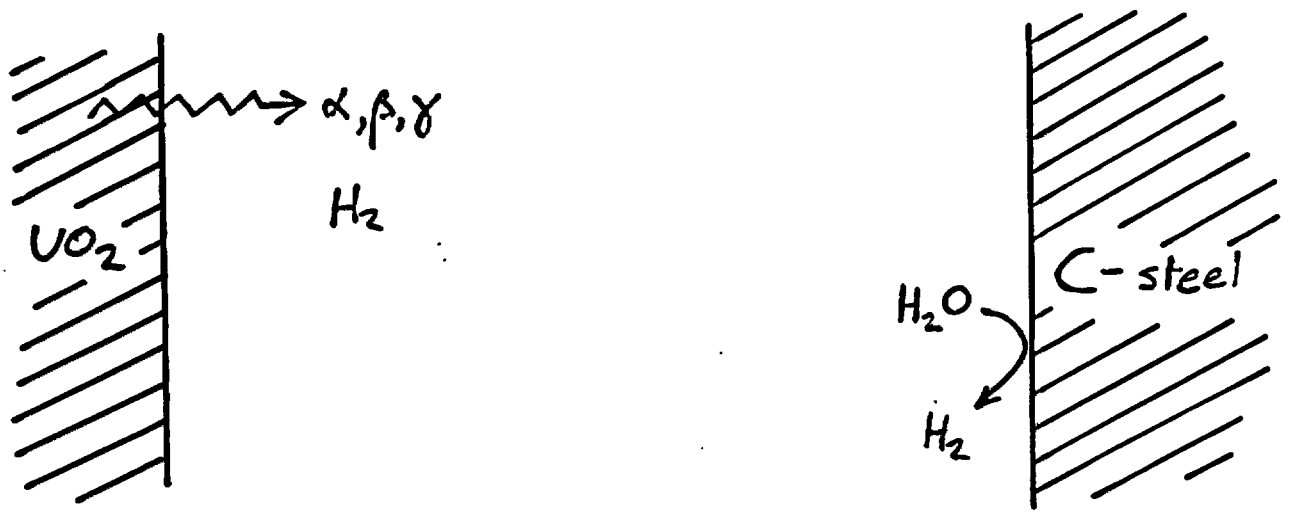

(4) Prediction of localized acidification and chemistry within deposits

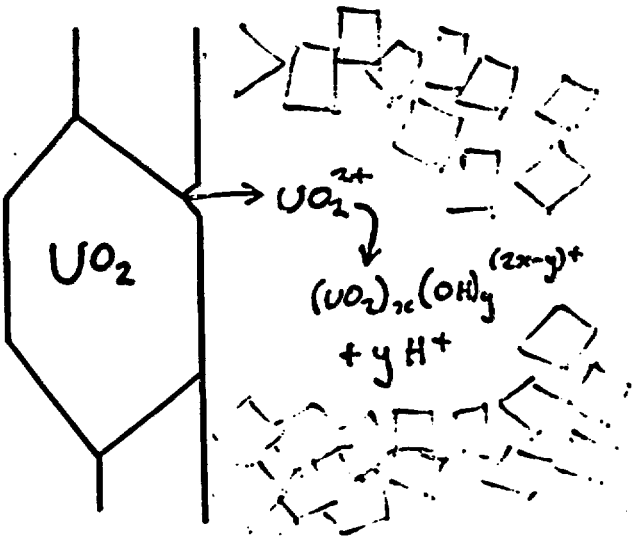

requires a radically different model

(5) Improvements to treatment of Fe_3O_4/Fe interface

Conclusions

- An electrochemically based model has been developed for predicting the effects of α-radiolysis, precipitation and redox reactions on the dissolution behaviour of used fuel.

- The reaction-diffusion of ten chemical species is included in the model (UO_2^{2+}, $UO_2(CO_3)_2^{2-}$, $UO_3 \cdot 2H_2O(s)$, CO_3^{2-}, O_2, H_2O_2, $Fe(II)_{AQ}$, $Fe(II)_{PPT}$, $U(IV)_{PPT}$ and $UO_2^{2+}(ads)$).

- The container/vault system is described by a 1-D system of porous mass-transport barriers representing corrosion product films, the container and buffer and backfill materials.

- The use of electrochemical boundary conditions permits the prediction of the corrosion potential (E_{CORR}) and dissolution rate (I_{CORR}) of both the UO_2 and C-steel surfaces.

- As yet, no predictions have been made!